geoconvention
Virtual Event
September 21-23
2020
CSPG · CSEG · CWLS · GAC · MAC · IAH

A new approach to visualize and interpret eigenvalues of Airborne Gravity Gradiometry (AGG) tensor data

Hassan H. Hassan and Serguei Goussev
Multiphysics Imaging Technology

Summary

With recent advances in the airborne gravity gradiometry (AGG) acquisition and processing, and the growing interest in their utilization in exploration for natural resources, it is becoming essential to develop new approaches for interpreting the AGG data. Gravity surveys, in general, measure variations in the Earth's gravity field, which is a function of the mass or density of subsurface rocks. Unlike the conventional airborne gravity data, interpretation of the AGG tensor data is more challenging because of its multicomponent nature. In the conventional airborne gravity surveys, a single component of the gravity field is measured: vertical component g_z. In contrast, AGG surveys measure nine components of the gravity gradient field along three mutually orthogonal x, y, and z directions. Together, the nine gravity gradients (T_{xx}, T_{yy}, T_{zz}, T_{xy}, T_{yx}, T_{xz}, T_{zx}, T_{yz}, and T_{zy}) form 3x3 symmetric second-rank traceless tensor. In the traceless tensor, sum of the diagonal elements is equal to zero (i.e., $T_{xx} + T_{yy} + T_{zz} = 0$). Among nine full tensor components, five are independent: T_{xx}, T_{yy}, T_{xy}, T_{xz}, and T_{yz}. The T_{zz} component is computed from T_{xx} and T_{yy} via the Laplace's equation. Since AGG measurements are made in a source-free space and in accordance with the Laplace's equation, $T_{zz} = -(T_{xx} + T_{yy})$. AGG surveys measure multiple components of the gravity field, and they provide a higher spatial resolution data than the conventional airborne gravity surveys. Moreover, AGG surveys measure the horizontal and the vertical gradients of the gravity field and, therefore, they are able to capture the high-frequency signals associated with shallow or near-surface geological targets. This is considered as one of the advantages of the AGG surveys over the conventional airborne surveys, because it provides an opportunity to map the ground water aquifers, near-surface mineral deposits, and shallow hydrocarbon accumulations. For the deep geological targets, perhaps, conventional airborne gravity surveys are more suitable, because the AGG signal loses its strength faster than a conventional gravity signal with the increasing depth: AGG signal strength diminishes by power of three, whereas the conventional gravity signal strength diminishes by power of two from the point sources. Tensor components of the AGG data (T_{xx}, T_{yy}, T_{zz}, T_{xy}, T_{xz}, and T_{yz}) provide useful information about geology of the area: gradient anomalies of the horizontal components (T_{xx}, T_{yy}, and T_{xy}) are related to the structural discontinuities such as faults, fractures, and lithological contacts. Vertical components of the AGG data (T_{zz}, T_{xz}, and T_{yz}) are related to the depth and density variations of the geological target. Generally, each of these six components is interpreted either separately or they are combined into a single image and interpreted as a single attribute. The latter approach is more appropriate in some cases, like interpreting the shape or curvature attributes of the geological target. In this study, we are introducing a new approach to interpret and visualize the AGG data based on combining the six tensor components (T_{xx}, T_{yy}, T_{zz}, T_{xy}, T_{xz}, and T_{yz}) into the single images describing shape and anisotropy attributes of the data. Using the six components of the AGG data, we computed three eigenvalues (λ_1, λ_2, and λ_3) from 3x3 Hessian matrix. The Hessian matrix is composed of the nine second-order derivatives of the gravity potential. Based on the three extracted eigenvalues, four shape and anisotropy attribute indices were computed using the eigenvalue magnitudes. These attribute indices are linear anisotropic (C_L), planar anisotropic (C_P), spherical anisotropic (C_S), and fractional anisotropic (FA). These attribute indices appear to be closely related to the rock density variations and structural geology of the area. We applied these attribute indices to the publicly available Falcon®

AGG data from the survey over the McFaulds Lake area in Ontario, Canada, to test their effectiveness in interpreting the AGG tensor data. The obtained results are, in general, intriguing and they show a good agreement between the degree of the tensor anisotropy, expressed by four anisotropic attribute indices, and the geological structure of the study area. It appears that the anisotropy is more intensive toward the western part of the study area, where most of the Precambrian rocks are located and subjected to the multiple phases of deformation, volcanism and mineralization.

Introduction

This study is describing a new approach to visualize and interpret the airborne gravity gradiometry (AGG) data acquired over the McFaulds Lake area (Fig. 1) in Ontario, Canada. AGG acquisition systems were developed by Bell Aerospace (currently, Lockheed Martin) for the US Navy. Initially, they were classified and used for the military applications. However, since their declassification in 1994, they have been used extensively for the mineral and oil explorations (Dransfield, 2007). Currently, there are two types of the commercial AGG systems in operation (DiFrancesco *et al.*, 2009): full tensor gravity gradiometer (FTG™) and partial tensor gravity gradiometer (Falcon®). The Falcon® system was developed as a joint venture between Lockheed Martin and BHP Billiton for the diamondiferous kimberlites exploration. Currently, Falcon® is used for both mineral and oil-and-gas exploration.

Figure 1. Study area.

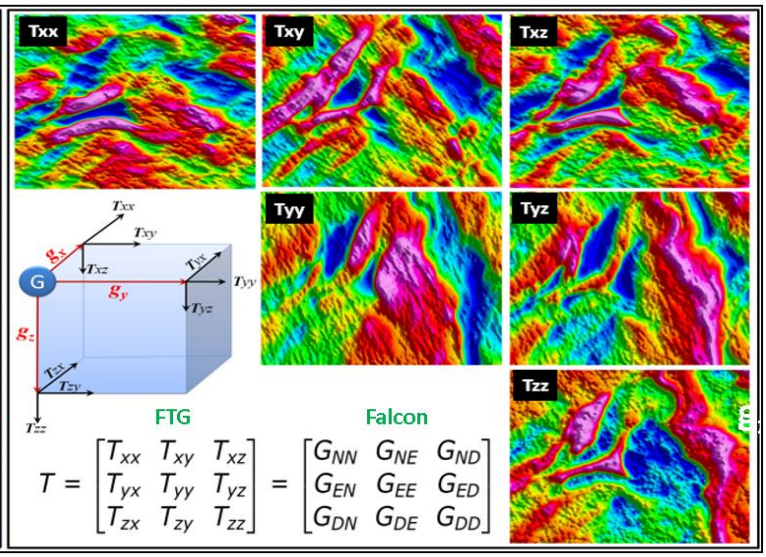

Figure 2. AGG tensor data over the McFaulds Lake.

The FTG™ system measures five independent gravity tensor components (T_{xx}, T_{xy}, T_{xz}, T_{yy}, and T_{yz}), from which T_{zz} is obtained via the Laplace's equation. For measurements made in the source-free space (i.e., air), second-order derivatives of the gravitational potential obey the Laplace's equation. Hence, the sum of T_{xx}, T_{yy}, and T_{zz} is equal to zero, so that $T_{zz} = - T_{xx} - T_{yy}$. The AGG tensor form a symmetric matrix with only six free second-order derivatives because the derivatives above and below its matrix diagonal are the same (Fig. 2).The Falcon system measures two curvature gradients G_{NE} and G_{UV}, from which other tensor components, such as G_{NN} (T_{xx}), G_{NE} (T_{xy}), G_{ND} (T_{xz}), G_{EE} (T_{yy}), G_{ED} (T_{yz}) and G_{DD} (T_{zz}), are derived by the Fourier transform or equivalent source technique (Fig. 2). Therefore, interpretation of the AGG data is, in general,

more complicated than interpreting the conventional gravity data, because the AGG data are composed of the six tensor components (T_{xx}, T_{xy}, T_{xz}, T_{yy}, T_{yz}, and T_{zz}).

There are two approaches to interpret the AGG data. One approach is to interpret each individual tensor component separately, and the other approach is to combine part or all the tensor components into a single attribute (for example, curvatures and rotational invariants) and interpret them accordingly (Dickson *et al.* 2009). This latter approach seems to be more effective in interpreting the AGG data, especially if the interpreter is interested in mapping the curvature attributes of the geological target. In this study, we are introducing a new concept to interpret the AGG data based on the use of the absolute values, or magnitudes, of three eigenvalues (λ_1, λ_2, and λ_3) computed from six components of the gradient tensor. Three eigenvalues and their corresponding eigenvectors can be used to estimate the shapes and anisotropic attributes of the geological targets in accordance with the concept of the tensor ellipsoid, or eigenvalue ellipsoid, whose three mutually orthogonal axial radii are defined by the eigenvalue magnitudes. Originally, this concept was developed for the MRI applications (Westin *et al.*, 1997; O'Donnell and Westin, 2011). Using three eigenvalues, we compute four anisotropic attribute indices: linear anisotropic (C_L), planar anisotropic (C_P), spherical anisotropic (C_S), and fractional anisotropic (FA) which was introduced by Basser and Pierpaoli (1996). Fractional anisotropic attribute index (FA) measures the deviation of the tensor ellipsoid shape from sphere. We also believe that FA can provide information about the structural framework and distribution of density contrasts in the study area.

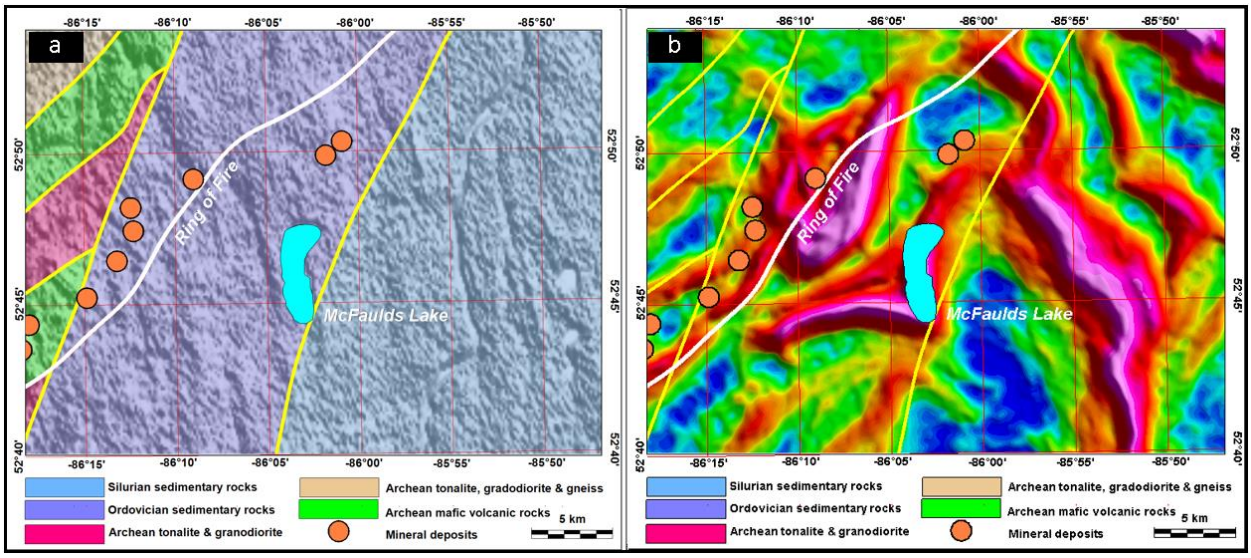

Figure 3. Generalized surface geology of the study area; (a) draped on topography; (b) plotted on top of horizontal gradient of the vertical gravity component g_z.

We applied four attribute indices to the publicly available Falcon® AGG data over part of the McFaulds Lake, Ontario, Canada (Fig. 1). The Falcon® survey was flown in 2011 by Fugro Airborne Surveys (currently CGG Multi-Physics) with 250m line spacing in the NW-SE direction and orthogonal tie lines with 2500m line spacing at the nominal terrain clearance of 100m. The Falcon® AGG dataset used in this study is shown in Figure 2. Geologically, the area is not well mapped, because it is covered by thick Quaternary rocks (Figure 3a). Regional mapping suggests that the Quaternary rocks overlay the highly deformed Precambrian ultramafic igneous rocks toward the western end of the study area with the younger Paleozoic sedimentary rocks in its

eastern part. Volcanogenic massif sulfide and chromite deposits are mined within the Precambrian ultramafic complex (Dyer and Burke, 2012). Figure 3b shows main geological elements of the study area plotted on top of the horizontal gradient of the vertical gravity component g_z.

Theory

The AGG tensor data T can be described by 3x3 Hessian matrix. Elements of the matrix represent the AGG tensor data, as shown below:

$$T = \begin{bmatrix} T_{xx} & T_{xy} & T_{xz} \\ T_{yx} & T_{yy} & T_{yz} \\ T_{zx} & T_{zy} & T_{zz} \end{bmatrix} \quad (1)$$

Diagonalization of the tensor T in Equation 1, yields a set of three eigenvalues (λ_1, λ_2, and λ_3) and their corresponding eigenvectors (ν_1, ν_2, *and* ν_3), respectively, along three principal orthogonal directions as expressed below:

$$T = [V] \,.\, [Q] \,.\, [V]^{-1} \quad (2)$$

Here, "Q" is the diagonal matrix that contains tensor eigenvalues at its diagonal. V is a vector that contains eigenvectors as shown below:

$$T = \begin{bmatrix} \nu_1 & \nu_2 & \nu_3 \end{bmatrix} \begin{bmatrix} \lambda_1 & 0 & 0 \\ 0 & \lambda_2 & 0 \\ 0 & 0 & \lambda_3 \end{bmatrix} \begin{bmatrix} \nu_1 & \nu_2 & \nu_3 \end{bmatrix}^{-1} \quad (3)$$

The eigenvalues carry information about the shape of the target, whereas the eigenvectors provide information related to orientation of three principal directions. In addition to providing the information related to the shape and orientation, eigenvalues and eigenvectors provide information related to the anisotropy of the target. Using the magnitudes of the eigenvalues λ_1, λ_2 and λ_3, we computed the linear anisotropic index (C_L), planar anisotropic index (C_P), spherical anisotropic index (C_S) and fractional anisotropic index (FA) as described on Figure 4. The linear, planar and spherical anisotropic indices were normalized by λ_1, so that their sum becomes equal to 1, and each individual index ranges from 0 to 1 (O'Donnell and Westin, 2011).

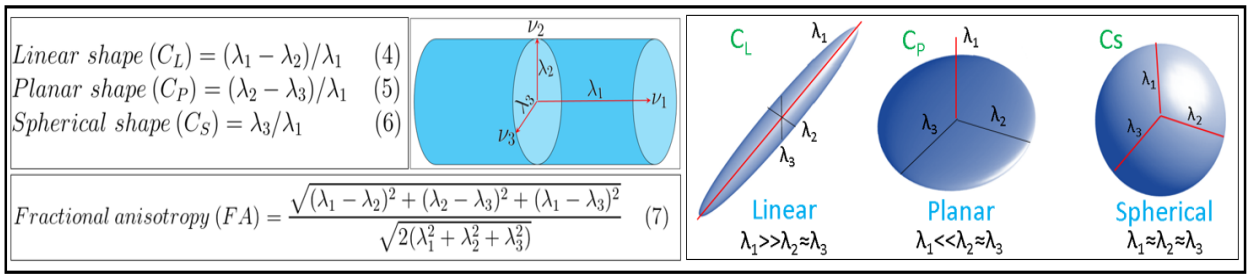

Figure 4. Anisotropic and shape attribute indices computed from a set of three eigenvalues λ1, λ2, and λ3

Examples

Falcon AGG tensor data (Fig. 2) for the McFaulds Lake area were used as input to compute three eigenvalues λ_1, λ_2, and λ_3. Afterward, we computed four shape and anisotropic attribute indices described in Figure 4 (C_L, C_P, C_S, and FA) using the equations 4, 5, 6, and 7, respectively.

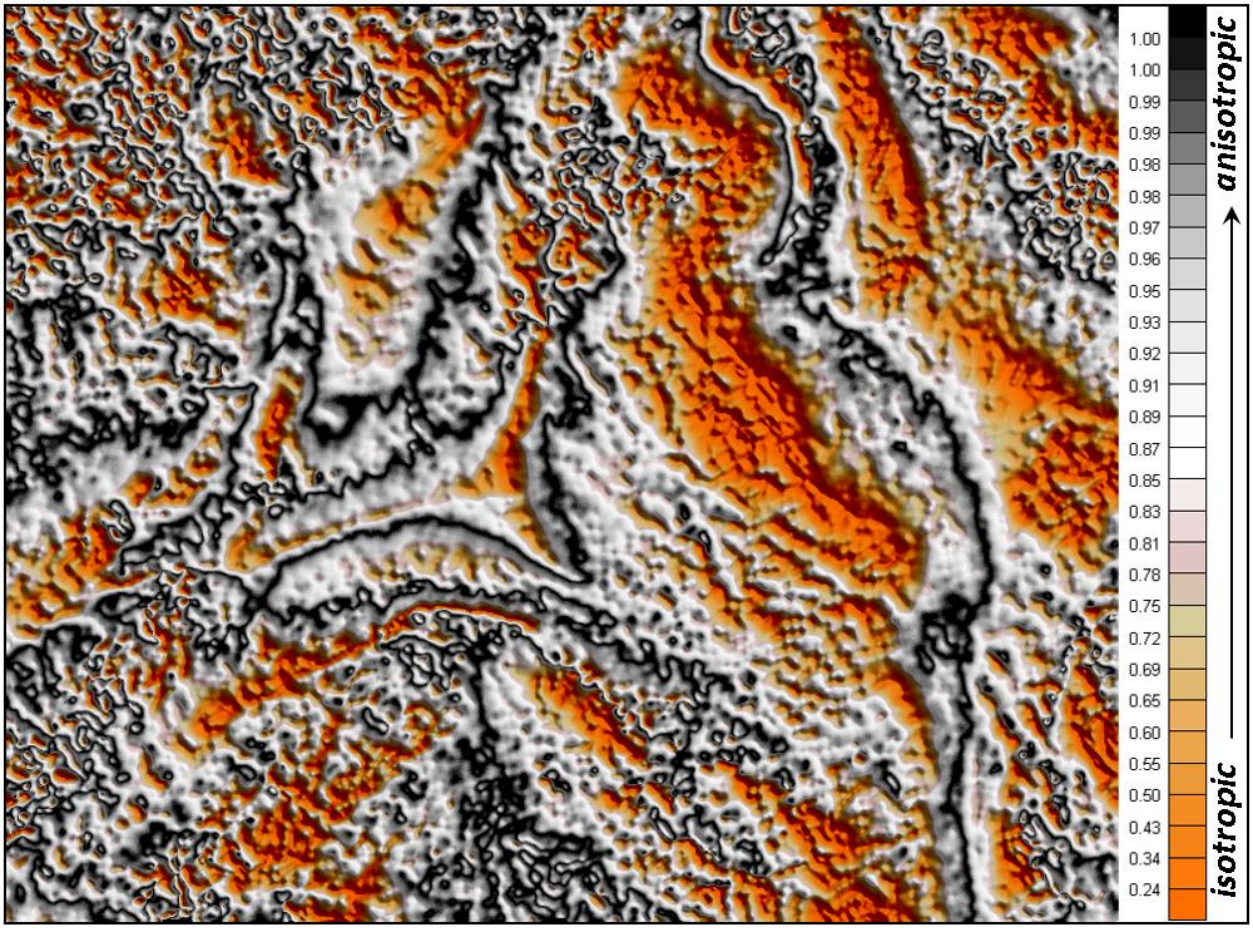

Figure 5. Fractional anisotropic attribute index (FA) map of the study area.

The result of calculating the fractional anisotropic attribute (FA) is displayed on Figure 5 which shows a fair agreement between the generalized geology of the area (Fig. 3) and the FA attribute alignments. It appears that strongly anisotropic areas on the FA image (black-color areas) coincide with the highly folded, faulted, and mineralized areas in the western part of the study area. In comparison to the horizontal gradient map (Fig. 3b), that is typically used for detection of faults, fractures and geological contacts, the FA map (Fig. 5) appears to be more resolving, and it shows elements of the subsurface structure of the area more clearly. In order to map the distribution of the tensor anisotropy parameters in the study area, we combined three anisotropic indices (i.e., C_L, C_P, and C_S) on the color-coded ternary plot (Fig. 6). It shows that the linear anisotropic index (magenta) is confined to the areas suspected to be highly deformed, whereas

the spherical isotropic (aqua) and planar anisotropic (yellow) indices appear to be confined to the areas with less deformation.

Conclusions

In this study, we introduced a new approach to interpret and visualize airborne gravity gradiometry (AGG) tensor data. This new approach takes advantage of both the ultra-high sensitivity of the tensor components to the spatial variations in distribution of density contrasts in subsurface and mathematical apparatus developed for the MRI applications. We use six tensor components of the AGG data to extract three tensor eigenvalues and compute four anisotropic indices using the eigenvalue magnitudes: linear anisotropic index (C_L), planar anisotropic index (C_P), spherical anisotropic index (C_S), and fractional anisotropic index (FA). These indices describe parameters of the tensor anisotropy in the study area that we believe are closely related to the rock density variations and provide an insight into the structural framework of the study area.

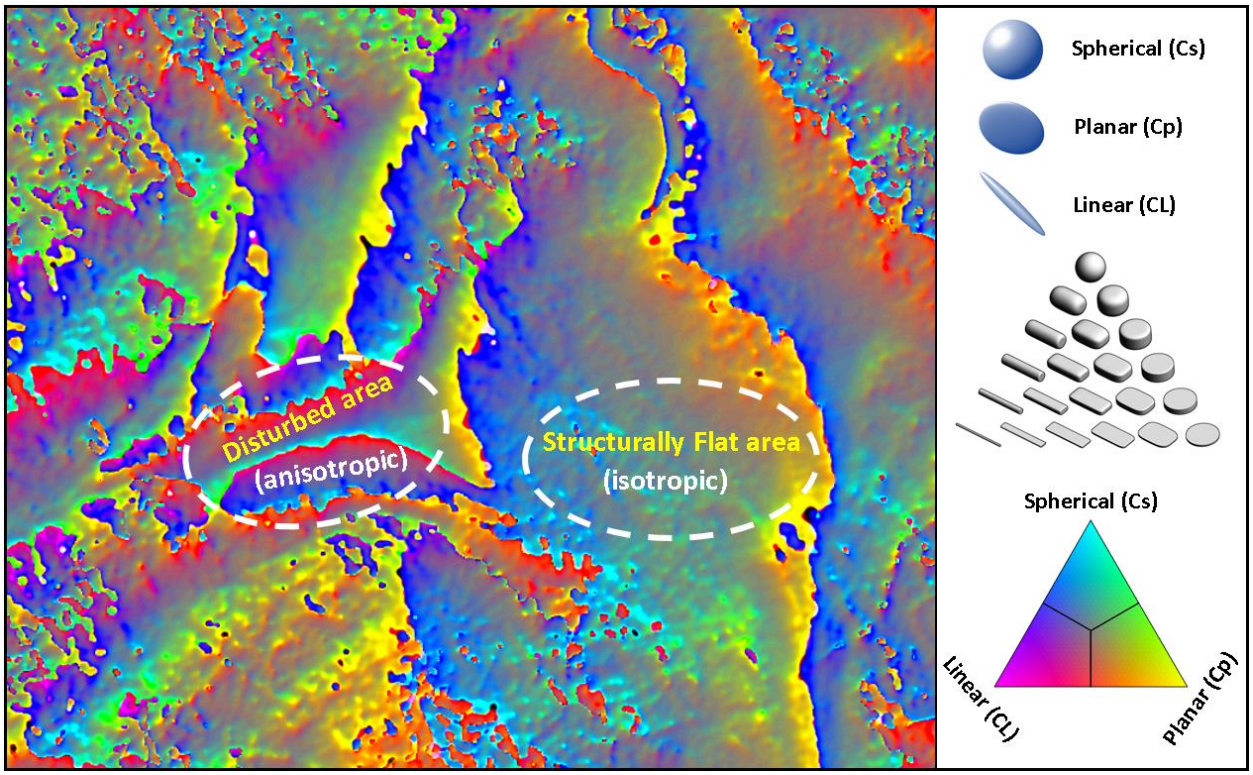

Figure 6. Ternary plot of the linear (C_L), planar (C_P), and the spherical (C_S) anisotropic indices.

References

Basser PJ, Pierpaoli C, 1996, Microstructural and physiological features of tissues elucidated by quantitative-diffusion-tensor MRI: Journal of Magnetic Resonance, Series B111, 209–219.

Dickinson, J. L., Brewster, J. R., and Murphy, C. A., 2009, imaging techniques for full tensor gravity gradiometry data: 11th SAGA Biennial Technical Meeting and Exhibition, Swaziland, 84-88.

DiFrancesco, D., Grierson, A., Kaputa, D., and Meyer, T., 2009, Gravity gradiometer systems – advances and challenges: Geophysical Prospecting, 57, 615–623

Dransfield, M.H., 2007, Airborne gravity gradiometry in the search for mineral deposits. *In* Milkereit, B. (Ed.) Proceedings of Exploration 07: Fifth Decennial International Conference on Mineral Exploration, 341-354.

Dyer, R.D. and Burke, H.E, 2012, Preliminary results from the McFaulds Lake ("Ring of Fire") area lake sediment geochemistry pilot study, northern Ontario: Ontario Geological Survey, Open File Report 6269, 26p.

O'Donnell, L.J., and Westin, C.F., 2011, An introduction to diffusion tensor image analysis: Neurosurgery Clinics of North America, 22, 185–196 viii.

Westin, C. F., Peled, S., Gubjartsson, H., Kikinis, R., and Jolesz, F. A., 1997, Geometrical diffusion measures for MRI from tensor basis analysis. In ISMRM, Conf. Proc., p.1742